



16 **Abstract**

17 Belowground autotrophic respiration (RA) is one of the largest, but highly uncertain carbon flux
18 components in terrestrial ecosystems. It has not been explored globally before and still acted as a “black
19 box” in global carbon cycling. Such progress and uncertainty motivate a development of global RA
20 dataset and understand its spatial and temporal pattern, causes and responses to future climate change.
21 This study used Random Forest to study RA’s spatial and temporal pattern at the global scale by linking
22 the updated field observations from Global Soil Respiration Database (v4) with global grid temperature,
23 precipitation and other environmental variables. Globally, mean RA was 43.8 ± 0.4 Pg C a⁻¹ with a
24 temporally increasing trend of 0.025 ± 0.006 Pg C a⁻¹ over 1980-2012. Such increment trend was widely
25 spread with 58% global land areas. For each 1 °C increase in annual mean temperature, global RA
26 increased by 0.85 ± 0.13 Pg C a⁻¹, and it was 0.17 ± 0.03 Pg C a⁻¹ for 10 mm increase in annual mean
27 precipitation, indicating a positive feedback of RA to future climate change. At a global scale,
28 precipitation was the main dominant climatic drivers of the spatial pattern of RA, accounting for 56% of
29 global land areas with widely spread globally, particularly in dry or semi-arid areas, followed by
30 shortwave radiation (25%) and temperature (19%). Different temporal patterns for varying climate zones
31 and biomes indicated uneven response of RA to future climate change, challenging the perspective that
32 the parameters of global carbon stimulation independent on climate zones and biomes. The developed
33 RA database, the missing carbon flux component that is not constrained and validated in terrestrial
34 ecosystem models and earth system models, will provide insights into understanding mechanisms
35 underlying the spatial and temporal variability of belowground carbon dynamics. RA database also has
36 great potentials to serve as a benchmark for future data-model comparisons. The RA product is freely
37 available at <https://doi.org/10.6084/m9.figshare.7636193>.

38

39

40

41



1 Introduction

Belowground autotrophic respiration (RA) mainly originated from plant roots, mycorrhizae, and other micro-organisms in the rhizosphere directly relying on labile carbon component leaked from roots
45 (Hanson et al., 2000; Tang et al., 2016; Wang and Yang, 2007). Thus, RA reflects the photosynthesis derived carbon respired back to atmosphere by roots and regulates the net photosynthetic production allocation to belowground tissues (Högberg et al., 2002). RA is also one main component of soil respiration (Hanson et al., 2000), which represents the second largest source of carbon fluxes from soil to the atmosphere (after gross primary production, GPP) in the global carbon cycle (Raich and
50 Schlesinger, 1992). Globally, RA contributed about 50% of total soil respiration on average, however, this contribution varied from 10% to 90% across biome, climate zones and among years (Hanson et al., 2000), leading to the strong spatial and temporal variability in biomes and climate regions. Thus global mean RA would amount from roughly 42 to 54 Pg C a⁻¹ (1 Pg = 10¹⁵ g) according to recent estimates of soil respiration (83-108 Pg C per year, Bond-Lamberty and Thomson, 2010b; Hursh et al., 2017), which
55 is almost 5 times of the carbon release from fossil fuel combustion from human activities (Le Quéré et al., 2017). Therefore, an accurate estimate of RA and its spatial-temporally dynamics is critical to understand the response of terrestrial ecosystems to global carbon cycling and climate change.

Due to the difficulties of separation and direct measurement of RA at varying spatial scales and its diurnal, seasonal and annual variabilities, RA becomes one of the largest but highly uncertain carbon flux
60 components in terrestrial ecosystems. Although individual site measurements of RA have been conducted across ecosystem types and biomes, knowledge gap still remains even though with a large number of field measurements (Hashimoto et al., 2015). Consequently, the globally spatial and temporal pattern of RA has not been explored and still acts as a “black box” in global carbon cycling. This “black box” is not well constrained and validated in most terrestrial ecosystem models and earth system models. Such
65 progress and uncertainty motivate a development of global RA dataset from observations and understand its spatial and temporal pattern, causes and responses to future climate change. Despite of the general agreement that global soil respiration increased during last several decades (Bond-Lamberty et al., 2018; Bond-Lamberty and Thomson, 2010b; Zhao et al., 2017), how global RA responding to climate change is far from certain because of different temperature sensitivities of RA across terrestrial ecosystems (Liu
70 et al., 2016; Wang et al., 2014). Therefore, reducing RA uncertainty and clarifying its response to climate



change, particularly to temperature and precipitation, is essential for global carbon allocation and future projection of climate change's effects on global terrestrial carbon cycle.

Although several studies have globally estimated soil respiration and its response to climate variables (Bond-Lamberty and Thomson, 2010b; Hursh et al., 2017; Zhao et al., 2017), such efforts have not been
75 conducted for global RA directly. Although Hashimoto et al. (2015) indirectly derived RA via the difference between total soil respiration and heterotrophic respiration, it probably led to uncertainty due to merely using the temperature and precipitation as the model drivers and a low model efficiency (32%). Besides temperature and precipitation, other variables, e.g. soil water, carbon and nitrogen content, are additionally critical factors regulating RA, and those factors generally varied with biomes and climate
80 zones. Consequently, Hashimoto et al. (2015) may not reflect the key processes affecting RA, such as soil nutrient limitation.

On the other hand, the climate-derived models usually explain < 50% variability of soil respiration (Bond-Lamberty and Thomson, 2010b; Hashimoto et al., 2015; Hursh et al., 2017), which might be another uncertainty source. Recent studies have included more variables and field observations to
85 promote the prediction ability of the linear or non-linear models (Jian et al., 2018; Zhao et al., 2017), yet it may propagate error because of the overfitting and autocorrelation among these variables (Long and Scott, 2006). Random Forest (RF, Breiman, 2001), a machine learning approach, could overcome these issues based on the hierarchical structure, and be insensitive to outliers and noise compared to single classifiers (Breiman, 2001; Tian et al., 2017). RF uses a large number of ensemble regression trees but a
90 random selection of predictive variables (Breiman, 2001). RF only requires two free parameter settings: the number of variables sampled as candidates for each split and the number of trees. The performance of the RF model usually is not sensitive to the number of trees and number of variables. Moreover, RF regression can deal with large number of features, and help feature selection based on importance and can avoid overfitting (Jian et al., 2018). RF has been widely used for carbon fluxes modelling in recent
95 years (Jung et al., 2017; Li et al., 2017; Zhao et al., 2017).

Therefore, this study firstly applied RF algorithm to retrieve global RA based on the updated RA field observations from the most updated global soil respiration dataset (SRDB, version 4, Bond-Lamberty and Thomson, 2010a) with the linkage of other global variables (see “materials and methods” part), aiming to: (1) develop a global RA product using field observations across the globe (named data-derived



100 RA); (2) estimate RA's spatial and temporal pattern; (3) identify the main driving factors of RA's spatial
and temporal variabilities; (4) compare with the previous RA estimates from Hashimoto et al. (2015).
The outcome of this study will advance our understanding of global RA and its spatial and temporal
variabilities. The proposed RA product is expected to serve as a benchmark for global vegetation models
and its role in global carbon cycling. It will also advance our knowledge of the co-variation of RA with
105 climate and other environmental factors, further link the empirical observations temporally and spatially
to bridge the knowledge gap among local, regional and global scales.

2 Material and methods

2.1 RA database development

First, RA database was developed based on observations across the globe from SRDB (Bond-Lamberty
110 and Thomson, 2010a), which is publicly available at <https://github.com/bpbond/srdb>. Then we further
updated the database using observations collected from China Knowledge Resource Integrated Database
(www.cnki.net) up to March 2018, which followed the identical criteria applied in SRDB development.
Annual RA observations were filtered that: (1) annual RA was directly reported in publications indicated
by "years of data" of SRDB; (2) the start and end years were recorded in literatures or expanded from
115 "years of data" of SRDB; (3) soil respiration measurements with Alkali absorption and soda lime were
not included due to the potential underestimate of respiration rate with the increasing pressure inside
chamber (Pumpanen et al., 2004); (4) observations with treatment of nitrogen addition, air/soil warming,
and rain/litter exclusion were not included, except cropland; (5) potential problems observations (labelled
by "Q10", "Q11", "Q12", "Q13" and "Q14") were excluded. Finally, this study included a total of 449
120 field observations (Fig. 1). RA observations were absolutely dominated by forest ecosystem (379
observations) with globally unevenly distributed, mainly from China, America and Europe. There was a
great lack of RA observations in Australia, Russia and Africa.

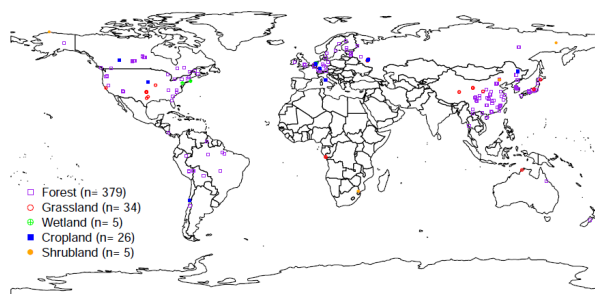


Figure 1 Observational sites used in this study

125 2.2 Vegetation, climate and soil data

Global land cover with a half degree resolution was obtained from MODIS land cover (<https://glcf.umd.edu/data/lc/>). Monthly grid data of temperature, precipitation, diurnal temperature range and potential evapotranspiration at 0.5° resolution were obtained from CRU TS Version 4.01 from 1901 to 2016 (<https://crudata.uea.ac.uk>) (Harris et al., 2014). Monthly shortwave radiation (SWR),
130 Palmer Drought Severity Index (PDSI) and soil water content at 0.5° resolution were from NOAA/ESRL Physical Sciences Division (<https://www.esrl.noaa.gov>) (Kalnay et al., 1996). Soil organic carbon content with a resolution of 250 m was downloaded from soil grid data (<https://soilgrids.org>) (Hengl et al., 2017), and soil nitrogen content was from Spatial Data Access Tool (<https://webmap.ornl.gov/ogc/index.jsp>), while monthly nitrogen deposition data with a resolution of 0.5° were downloaded from the Earth System
135 Models of GISS-E2-R, CCSM-CAM3.5 and GFDL-AM3, covering since 1850s (<https://www.isimip.org>). The monthly global variables were first aggregated to year scale and then resampled to a 0.5° resolution using bilinear interpolation for those variables without a 0.5° resolution. These variables could represent different aspects controlling RA variability. For instance, temperature, precipitation and soil water content are most important variables controlling plant photosynthesis, which
140 is the primary carbon source of RA (Högberg et al., 2002; Högberg et al., 2001). Finally, global variables of each given site extracted by coordinates corresponding with annual RA estimates from the SRDB.

2.3 Random Forest-based RA Modelling

In this study, a RF model was trained with the 11 variables listed in Table S1 by *caret* by linking *RandomForest* package in R 3.4.4 (Kabacoff, 2015), then the trained model was implemented to estimate



145 grid RA at $0.5^\circ \times 0.5^\circ$ resolution over 1980-2012. The performance of RF was assessed by a 10-fold cross-validation (CV). A 10-fold CV suggested that the whole dataset was subdivided into 10 parts with approximately an equal number of samples. The target values for each of these 10 parts were predicted on the training using the remaining nine parts. Two statistics were employed in model assessment: modelling efficiency (R^2) and root mean square error ($RMSE$) (Yao et al., 2018). The 10-fold CV result
150 showed that RF performed well and could capture the spatial- and temporal-pattern of RA (Fig. S1 in supplementary materials).

2.4 Temporal trend analysis

This study applied Theil-Sen linear regression to estimate temporal trend analysis of RA and its driving variables for each grid cell. The Theil-Sen estimator is a median-based non-parametric slope estimator,
155 which has been widely used for spatial analysis of time series carbon flux (Forkel et al., 2016; Zhang et al., 2017). Mann-kendall non-parametric test was applied for the significant change trend in RA and its driving factors for each grid cell ($p < 0.05$).

2.5 Relationships between RA and climate variables

In this study, mean annual temperature, mean annual precipitation and mean annual shortwave radiation
160 were considered as the most important proxies driving RA. The relationships between RA and temperature, precipitation and shortwave radiation were analyzed by partial correlation for each grid cell. The absolute value of the correlation coefficient of these three variables was used in RGB combination to indicate the dominant factors of RA.

2.6 The comparison map profile method

165 In order to compare with the solely global RA product generated by (Hashimoto et al., 2015), this study applied the comparison map profile (CMP) method. CMP was developed based on absolute distance (D) and cross-correlation coefficient (CC) through multiple scales (Gaucherel et al., 2008). D and CC reflect the similarity of data value and spatial structure of two images with the same size, respectively (Gaucherel et al., 2008). Low D and higher CC reflects goodness between the compared images, and vice
170 versa. The D among moving windows of two compared images was calculated by equation (1) (Gaucherel et al., 2008):



$$D = \text{abs}(\bar{x} - \bar{y}) \quad (1)$$

\bar{x} and \bar{y} are averages calculated over two moving windows. This study used 3×3 to 41×41 pixels.

Finally, the mean D was averaged for different scales.

175 The CC was calculated by equation (2) (Gaucherel et al., 2008):

$$CC = \frac{1}{N^2} \sum_{i=1}^N \sum_{j=1}^N \frac{(x_{ij} - \bar{x})(y_{ij} - \bar{y})}{\sigma_x \sigma_y} \quad (2)$$

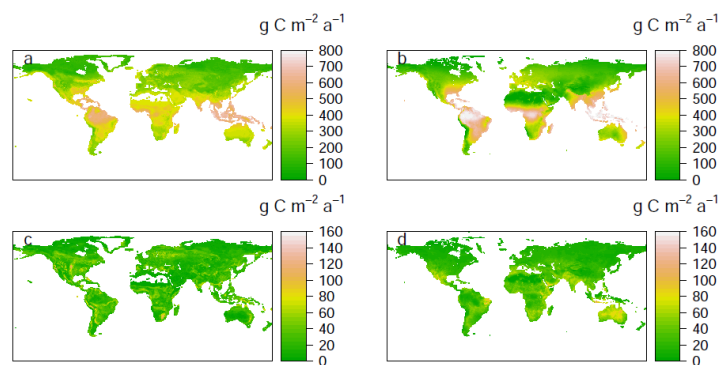
$$\text{With } \sigma_x^2 = \frac{1}{N^2 - 1} \sum_{i=1}^N \sum_{j=1}^N (x_{ij} - \bar{x})^2 \quad (3)$$

Where x_{ij} and y_{ij} are the pixel values at row i and column j of two moving windows of the two compared images, respectively. N represents the number of pixels for each moving window, while σ_x and σ_y are the

180 standard deviation calculated from the two moving windows. Finally, like D calculations, CC were calculated as the mean of different scales.

3 Results

3.1 Spatial patterns of RA



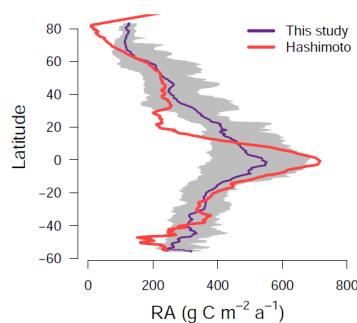
185 **Figure 2** Spatial patterns of annual mean (a, b) and standard deviation (c, d) of belowground autotrophic respiration (RA) for this study (a, c) and Hashimoto RA (b, d) during 1980-2012.

The data-derived RA in this study presented a great globally spatial variability during 1980-2012 (Fig. 2a and Fig. 3). Largest RA fluxes commenced from tropical regions, particularly in Amazon tropical and Southeast areas where generally have a high RA > 700 g C m⁻² a⁻¹. Following the tropical areas, subtropics, e.g. South China, East America, and humid temperate areas, e.g. North America, West and Middle Europe,

190



had typical moderate RA fluxes of 400-600 g C m⁻² a⁻¹. By contrast, relative low RA fluxes occurred in the areas with sparse vegetation cover, cold and dry climate, e.g. boreal and tundra, which had low temperature and short growing season. Besides, dry or semi-arid areas, e.g. Northwest China and Middle East, also had typical low RA fluxes below 200 g C m⁻² a⁻¹, where were often limited by water availability.



195

Figure 3 Latitudinal pattern of belowground autotrophic respiration (RA) for this study and Hashimoto RA. The grey area means 2.5 to 97.5 percentile ranges of the predicted RA.

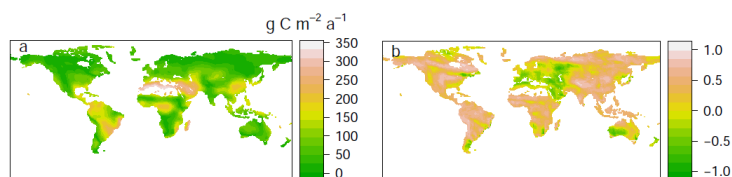
The most significant RA variability (expressed by standard deviation, Fig. 2c) was found in tropical or subtropical regions with above 80 g C m⁻² a⁻¹, while most areas remained less variable with less than 40 g C m⁻² a⁻¹. Latitudinally, zonal mean RA increased from cold and dry biomes (Tundra and semi-arid) to warm and humid biomes (temperate and tropical forests, Fig. 3), reflecting from more to less environmental limitations. RA varied from 112±21 g C m⁻² a⁻¹ at about 70°N to 552±101 g C m⁻² a⁻¹ at equator. Within in 10°S -25°S and 15°N -20°N, due to the limitation of water, zonal mean RA experienced a slight decrease. Therefore, with the increase of water availability, RA led to a second peak in around 20°N and 40°S, respectively.

Compared to data-derived RA, Hashimoto RA presented a similar spatial pattern, with highest RA fluxes in tropical regions characterized by warm and humid climate, followed by subtropical regions, and lowest RA in boreal areas featured by in cold and dry climate (Fig. 2b). The most significant change occurred in tropical areas and middle Australia. However, it is worth noted that some clear differences between data-derived and Hashimoto RA existed (Fig. 4): specifically, there was a remarkable difference of above 300 g C m⁻² a⁻¹ for South Amazon and larger than 200 g C m⁻² a⁻¹ for subtropical China. Although most areas between data-derived RA and Hashimoto RA expressed high and positive correlations, some areas,

210

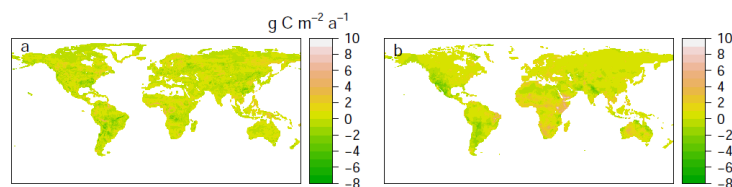


such as Middle East, West Russia and East America and North Japan, showed negative correlations.



215 **Figure 4** Comparison of data-derived RA with Hashimoto RA based on absolute distance (a) and cross-
correlation (b)

3.2 | Spatial pattern of RA trend



220 **Figure 5** Spatial patterns of the temporal trend for belowground autotrophic respiration (RA) for this
study and Hashimoto RA during 1980-2012

The trend of data-derived RA showed heterogeneous patterns in spatial (Fig. 5). A total of 58% of global areas experienced an increasing trend during 1980-2012 (calculating from cell areas), and 33% of these areas showed a significant change ($p < 0.05$). Generally, the change trend for the majority areas was within $-4 - 4 \text{ g C m}^{-2} \text{ a}^{-1}$, while the most striking increasing change occurred in East Russia and tropical and Eastern regions in Africa with an increasing trend of above $5 \text{ g C m}^{-2} \text{ a}^{-1}$. Similarly, 77% of global areas of Hashimoto RA had an increasing trend, 46% of which were statistically significant ($p < 0.05$).

3.4 | Total RA and its temporal trend

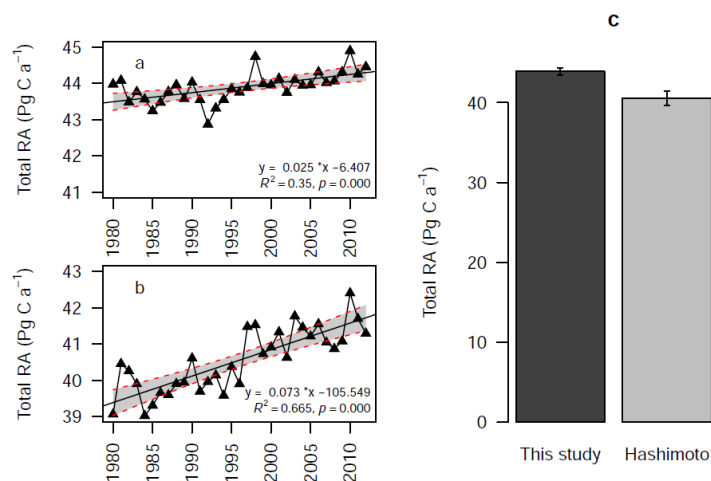


Figure 6 Inter-annual variability (a and b) and total amount (c) of belowground autotrophic respiration (RA) for this study and Hashimoto RA during 1980-2012. The grey area represents 95% confidence interval. The error bars mean standard deviation.

Mean global RA was $43.8 \pm 0.4 \text{ Pg C a}^{-1}$ during 1980-2012 (Fig. 6c), varying from 42.9 Pg C a^{-1} in 1992 to 44.9 Pg C a^{-1} in 2010, with a significant trend of $0.025 \pm 0.006 \text{ Pg C}$ per year despite of high annual variabilities ($0.06\% \text{ a}^{-1}$, $p < 0.001$, Fig. 6a). Similarly, a rising trend was also observed for Hashimoto RA, however, its annual increasing trend ($0.073 \pm 0.009 \text{ Pg C a}^{-1}$, $p < 0.001$, Fig. 6b) was higher than that of data-derived RA. Annual mean of Hashimoto RA was $40.5 \pm 0.9 \text{ Pg C a}^{-1}$ (Fig. 6c).

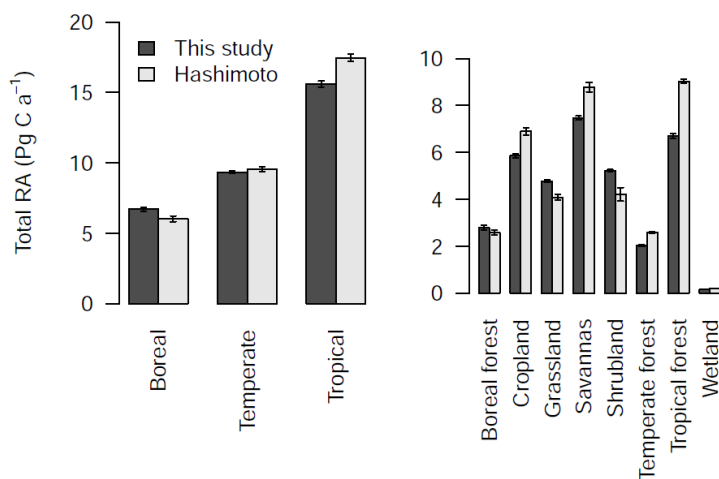




Figure 7 Total amount of belowground autotrophic respiration (RA) for this study and Hashimoto RA for three climate zones and eight biomes during 1980-2012. Three climate zones defined as boreal, 240 temperature and tropical regions according to Peel et al. (2007), while eight biomes include boreal forest, cropland, grassland, savannas, shrubland, temperate forest, tropical forest and wetland. The error bars indicated standard deviation.

RA and its trend was also evaluated for three climate zones (boreal, temperal and tropical areas based on Köppen-Geiger climate classification) and eight major biomes (boreal forest, cropland, grassland, 245 savannas, shrubland, temperate forest, tropical forest and wetland, Fig. 7). Tropics had highest RA of $15.6 \pm 0.2 \text{ Pg C a}^{-1}$, followed by temperate regions with $9.3 \pm 0.1 \text{ Pg C a}^{-1}$, and boreal areas represented the lowest RA of $6.7 \pm 0.1 \text{ Pg C a}^{-1}$. These three climate zones were main contributors of global RA, accounting for 72%. Temporally, considerable RA inter-annual variability of these three climate zones existed (Fig. S2). Specifically, RA in tropical and boreal zones showed a significantly increasing trend 250 from 1980 to 2012, with an increasing rate of 0.013 ± 0.003 and $0.008 \pm 0.002 \text{ Pg C a}^{-1}$. However, RA in temperate zones presented a slightly decreasing trend of $-0.003 \pm 0.001 \text{ Pg C a}^{-1}$ ($p = 0.048$) although strong variability was observed.

In terms of biomes, tropical forest had the highest RA, followed by the widely distributed cropland and savannas (Fig. 7), while wetland had the lowest RA due to its limited land cover. All the biomes, except 255 temperate forest, savannas and wetland, showed a significantly increasing trend during 1980-2012 ($p_s < 0.05$). Tropical forest, boreal forests and cropland had the highest increasing trend of 0.0076 ± 0.0015 , 0.0047 ± 0.0016 , $0.0036 \pm 0.0014 \text{ Pg C a}^{-1}$, respectively. Compared to data-derived RA, Hashimoto RA for the three climate zones and eight biomes generally produced similar change patterns, although the magnitude difference existed (Figs. 7, S2 and S3). However, there was a significant increasing trend of 260 temperate zones, temperate forest, savannas and wetland for derived from Hashimoto RA, which were not observed in data-derived RA.

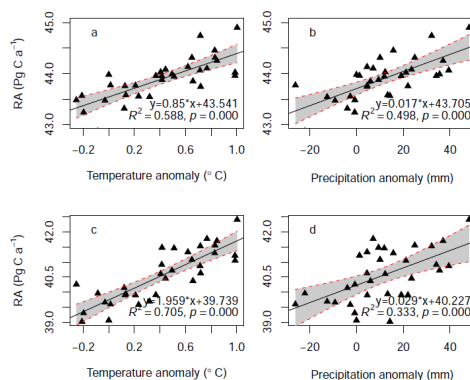


Figure 8 The relationships between belowground autotrophic respiration (RA) and the anomaly of temperature and precipitation for this study (a, b) and Hashimoto (c, d) respectively. The anomaly was calculated as the difference between temperature or precipitation of corresponding year to that of 1980.

RA was significantly correlated with temperature anomaly ($R^2 = 0.59$, $p < 0.001$) and precipitation anomaly ($R^2 = 0.50$, $p < 0.001$, Fig. 8). On average, RA increased by 0.85 ± 0.13 Pg C a⁻¹ for 1°C increment in mean annual temperature, and 0.17 ± 0.03 Pg C a⁻¹ for 10 mm increase in mean annual precipitation. However, different biomes and climate zones showed uneven responses to the temperature and precipitation change (Fig. S4 and S5). For example, no significant correlations were found between RA in temperate zone/savannas/wetland and temperature anomaly, while other climate zones and biomes were significantly correlated with temperature/precipitation anomaly.

4. Dominant factors for RA variability

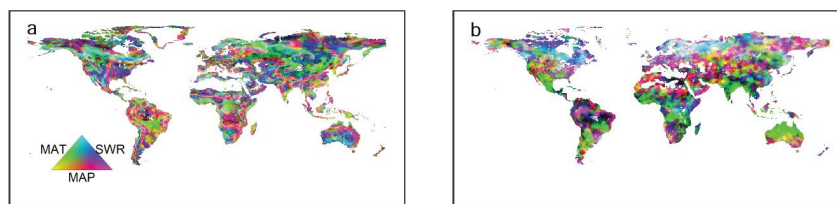


Figure 9 Dominant factors for belowground autotrophic respiration (RA) for this study and Hashimoto RA. MAT = mean annual temperature, MAP = mean annual precipitation; SWR = shortwave radiation.

The dominant environmental factor was examined with partial regression coefficients when regressing RA against annual mean temperature, annual mean precipitation and shortwave radiation. Latitudinally,



higher mean annual temperature, precipitation and shortwave radiation were associated with higher RA
280 in the major latitudinal gradients (positive partial correlations, Fig. S6). Spatially, the dominant
environmental factor varied greatly globally (Fig. 9). Precipitation was the most important dominant
factor for the spatial pattern of RA among the three environmental controls, covering about 56% of global
land areas (Fig. S7), which was widely distributed globally, particularly in dry or semi-arid areas, such
as Northwest China, Southern Africa, Middle Australia and America. Temperature dominated about 19%
285 of global land areas, which mainly occurred in tropical Africa, Southern Amazon rainforests, Siberia and
partly tundra. The rest land area (25%) was dominated by shortwave radiation, primarily covering boreal
areas above 50°N, Eastern America and middle and Eastern Russian. Similarly, precipitation was also the
most important dominant factor for Hashimoto RA, dominating about 77% land area, while temperature
and shortwave radiation dominated 13% and 10% land area. However, their spatial patterns varied greatly
290 compared to data-derived RA. For example, temperature was the main dominant factor for most area of
Australia, while data-derived RA indicated that precipitation and shortwave radiation dominated such
areas (Fig. 9).

4 Discussion

4.1 Global RA

295 Despite of great efforts to quantify global soil carbon fluxes and their spatial and temporal patterns
(Bond-Lamberty and Thomson, 2010b; Hursh et al., 2017; Jian et al., 2018), to our knowledge, no attempt
tried to assess RA using machine learning approach by linking a large number of empirical measurements,
and RA's spatial and temporal patterns remain large uncertainties. Such uncertainties justify a
development of global RA product derived from observations to understand its spatial and temporal
300 patterns, causes and responses to future climate change. Based on the most updated observations from
SRDB released by the end of 2018, this study for the first time applied RF algorithm to estimate the
temporal and spatial variability of global RA and its response to environmental variables, which indeed
can contribute to reduce RA uncertainties.

Globally, mean annual RA amounted to 43.8 ± 0.4 Pg C a⁻¹ from 1980 to 2012 (Fig. 6). It was slightly
305 higher than Hashimoto RA (40.5 ± 0.9 Pg C a⁻¹), and there was great divergence of spatial and temporal
patterns (see discussion part in “*Comparison with Hashimoto RA*”). Due to no direct estimate on global



RA, this study compared other RA estimates using total soil respiration multiplied by the proportion of RA or heterotrophic respiration. Bond-Lamberty et al. (2018) proposed that the global average proportion of heterotrophic respiration ranged from 0.54 to 0.63 over 1990-2014 and global total soil respiration was 83 to 108 Pg C a⁻¹ from different approaches according to recent predictions (Bond-Lamberty and Thomson, 2010b; Hursh et al., 2017), thus global RA varied from 31 to 51 Pg C a⁻¹. RA estimate in this study fell in this range. Similarly, during 1980-2012, RA increased by 0.025±0.006 Pg C a⁻¹, which may be related to the increasing photosynthesis due to global warming and CO₂ fertilization effects, which could increase carbon availability in plant-derived substrate inputs into the soil (e.g. root exudates and biomass) for both root metabolism (Piñeiro et al., 2017; Zhou et al., 2016). Such annual increase accounted for about 25% of global soil respiration increase (0.09 and 0.1 Pg C a⁻¹) (Bond-Lamberty and Thomson, 2010b; Hashimoto et al., 2015), suggesting that about one quarter of the total soil respiration increment due to climate change came from RA. With 1 °C increase in global mean temperature, RA will increase by 0.85±0.13 Pg C a⁻¹ and 0.17±0.03 Pg C a⁻¹ for 10 mm increase in precipitation, which indicated that carbon fluxes from RA might positively feedback to future global climate change, which was typically characterized by increasing temperature and changes in precipitation (IPCC, 2013).

RA estimate in this study also has important indications of carbon allocation from photosynthesis. The immediate carbon substrates for RA were primarily derived from recent photosynthesis (Högberg et al., 2001; Subke et al., 2011). Strong correlation between photosynthesis and RA demonstrated the evidence for their close coupling relationships (Chen et al., 2014; Kuzyakov and Gavrichkova, 2010). Globally, GPP was about 125 Pg C a⁻¹ during last few decades (Bodesheim et al., 2018; Zhang et al., 2017). Thus, roots respired more than one third carbon from GPP, suggesting that except the carbon used for constructing belowground tissues, a large proportion of carbon will be returned back to atmosphere respired by roots. However, it should be noted that through root respiration, soil nutrients for vegetation growth will be required, which may affect the RA flux.

4.2 Dominant factors

Spatially, the driving factors for RA varied greatly. Temperature and shortwave radiation were the main driving factors for high latitudinal areas above 50°N (Figure 9a). This result was not surprising because RA was positively correlated with temperature or photosynthesis (indirectly reflecting the solar radiation) (Chen et al., 2014; Tang et al., 2016), and high latitudinal regions was always limited by temperature or



energy, leading to low RA as well (Fig. 3a).

Globally, precipitation was the most important factor, covering about 56% of land area (Fig. 9a and S7). Precipitation was always considered as a proxy for soil water content (Hursh et al., 2017; Yao et al., 2018), and such wide dominance of precipitation on RA was related to the mechanisms of the soil water availability driving RA. First, soil water exists in form of ice when temperature is below zero, that plant and soil microbes could not directly use for growth or respiration. This could be observed in some boreal areas where precipitation was the dominant factor of RA (Fig. 9a). Second, too high or too low soil water content (e.g. flooding and drought) could limit the mobility of substrates and carbon input to belowground, which could affect RA. Yan et al. (2014) found that soil respiration decreased once soil water content was below a lower (14.8 %) or above an upper (26.2%) threshold in a poplar plantation. Similarly, Gomez-Casnovas et al. (2012) also found that RA decreased when soil water content was above 30%. These results seemed to support the finding in this study. Third, the relationship between soil water content and RA or total soil respiration is more complex than the relationship between temperature and soil respiration. Numerous formula, such as linear (Tang et al., 2016), polynomial (Moyano et al., 2012), logarithmic (Schaefer et al., 2009), quadratic (Hursh et al., 2017) models have been widely applied to describe the relationship between soil water content and soil respiration. The multifarious relationships between soil water content and RA may occur because soil water content affect RA in multiple ways. Meanwhile, seasonal variability of precipitation and soil water content is often correlated with temperature (Feng and Liu, 2015), making the relationship between soil water content and RA more complex.

Similarly, the dominance of precipitation in Hashimoto was also widely observed (Fig. 8), dominating 77% of land area (Fig. S7). Although this percentage was 17% higher than data-derived RA, both results demonstrated that global RA of the majority land cover was dominated by precipitation. However, it is noticeable that dominant environmental factor controlling spatial carbon fluxes gradient may differ among different years (Reichstein et al., 2007), e.g. climate extreme and disturbance.

4.3 Comparison with Hashimoto RA

Globally, total data-derived RA was slightly higher than Hashimoto RA, however, great divergence was observed both spatially and temporally (Fig. 6), particularly in tropical regions, where data-derived RA was much lower than Hashimoto RA (Fig. 3). These differences could be attributed to several reasons.



365 First, two RA products had different land cover areas, especially in desert areas in North Africa, where
existed very sparse or no vegetation. If data-derived RA was masked by Hashimoto RA, global RA was
39.6±0.4 Pg C a⁻¹, which was pretty close to Hashimoto RA (Fig. S8). Second, different predictors and
algorithms were applied for data-derived RA and Hashimoto RA prediction. Besides temperature and
precipitation, RA was also affected by soil nutrient, carbon substrate supply, belowground carbon
370 allocation, site disturbance and other variables (Chen et al., 2014; Hashimoto et al., 2015; Tang et al.,
2016; Zhou et al., 2016). Hashimoto RA was calculated from the difference between total soil respiration
and heterotrophic respiration, which were predicted by a simple climate-driven model using temperature
and precipitation only (Hashimoto et al., 2015). Thus Hashimoto RA could not reflect its soil nutrient
and other environmental constrains. To overcome such limitations, beside temperature and precipitation,
375 this study included soil water content, soil nitrogen and soil organic carbon as proxies for environmental
and nutrient constraints of RA and considered the interactions among these variables using RF. This study
indeed improved the model efficiency to 0.52 for RA prediction (Fig. S1), which was 0.32 for Hashimoto
soil respiration (Hashimoto et al., 2015). The simple climate-model for Hashimoto soil respiration could
be its advantages and limitations (Hashimoto et al., 2015). Third, the empirical model (the relationship
380 between total soil respiration and heterotrophic respiration) deriving Hashimoto RA originated from
forest ecosystems (Bond-Lamberty et al., 2004; Hashimoto et al., 2015), which may bring uncertainties
to other ecosystems. For example, the difference between data-derived RA and Hashimoto RA varied up
to 350 g C a⁻¹ in South, North Amazon areas and Madagascar, where the savannas widely distributed
(Fig. 4), thus Hashimoto RA might not capture the spatial and temporal pattern of RA for non-forest
385 ecosystems. Including more environmental variables and improving algorithm could be a good option to
reduce the uncertainty in modelling RA.

4.4 Advantages, limitations and uncertainties

Generally, this study had four main advantages to estimate global RA: first, this study, to our knowledge,
was the first attempt to model RA using a large number of empirical field observations, and estimate
390 spatial and temporal patterns globally. While most previous studies mainly focused on global total soil
respiration, which was not partitioned into RA and heterotrophic respiration globally (Hursh et al., 2017;
Jian et al., 2018; Zhao et al., 2017). Second, this study used an up-to-date field observational database
developed from SRDB up to the end 2018. This new updated database included a total of 449 field



observations (Fig. 1). These observations had a wide coverage range of global terrestrial ecosystems and
395 represented all major biomes and climate zones. Third, the global terrestrial ecosystems were separated
into eight biomes, including boreal forest, cropland, grassland, savannas, shrubland, temperate forest,
tropical forest and wetland. The total RA and its inter-annual variability were evaluated for each of the
eight biomes (Fig. S3 and S4). Besides, total RA and its inter-annual variability was also assessed for
three climate zones - boreal, temperate and tropical zones (Figs. S2 and S5), according to the Köppen-
400 Geiger climate classification system (Peel et al., 2007). These were important climate zones, contributing
72% of global RA. Different temporal change trends across biomes and climate zones also further
indicated an uneven response of RA to climate change. Fourth, this study used a RF algorithm to model
and map global RA with the linkage of climate and soil predictors. The results showed that RF could
accurately estimate the relationships between annual RA and predictors (Fig. S1). Compared to linear
405 regressions for soil respiration prediction (because no global RA prediction before this study) with a
model efficiency less than 35% (Bond-Lamberty and Thomson, 2010b; Hashimoto et al., 2015; Hursh et
al., 2017), RF algorithm achieved a much higher model efficiency to 52%, which indeed improved the
RA modelling and reduced the uncertainties.

Although data-derived global RA could serve as a benchmark for global carbon cycling modelling, and
410 this study had filled the data-gaps of global RA, limitations and uncertainties still remained in few aspects.
First, the effects of rising atmospheric CO₂ on root growth was not explicitly represented in this study,
although CO₂ fertilization effects could partly be represented in the increase temperature. While the
magnitude of CO₂ fertilization effects on photosynthesis is still uncertain (Gray et al., 2016), RF or other
machine learning approaches are encouraged to quantify the uncertainties due to CO₂ fertilization.
415 Second, this study did not consider the effects of human activities and historical changes in biomes on
RA. However, important changes may occur in tropical forest, grassland and cropland during last several
decades due to human activities (Hansen et al., 2013; Klein Goldewijk et al., 2011). Thus, changes in
biomes should be included in future global RA and carbon cycling modelling. However, the lack of such
data is the main constrain of detecting the effects of biome change on RA. Third, uneven coverage of
420 observations in the updated database would be another source of uncertainties. Although our dataset had
a wide range of land cover, the observational sites mainly distributed in China, Europe and North America
and were dominated by forests. There was a great lack of observations in areas, such as Africa, Austria



and Russia, and biomes, such as tropical forest, shrubland, wetland and cropland. Therefore, including
more observations in these areas and biomes should largely increase our capability to assess the spatial
425 and temporal patterns of global RA and contribute to improve the global carbon cycling modelling to
future climate change.

5 Data availability

The datasets are freely downloadable from <https://doi.org/10.6084/m9.figshare.7636193> (Tang et al.,
2019).

430 6 Conclusions

Although data-derived global RA may serve as a benchmark for ecosystem models, no such study has
assessed global variability in RA with a large number of empirical observations that can help bridge the
knowledge gap between local, regional, and global scales. This study has filled this knowledge gap by
linkage of field observations and global variables using RF algorithm, providing an annual global RA
435 product at a of $0.5^\circ \times 0.5^\circ$ resolution from 1980 to 2012. Currently, robust findings include: (1) Annual
mean RA was $43.8 \pm 0.4 \text{ Pg C a}^{-1}$ with a temporally increasing trend of $0.025 \pm 0.006 \text{ Pg C a}^{-1}$ over 1980-
2012, indicating an increasing carbon return from the roots to the atmosphere; (2) uneven temporal and
spatial variabilities in varying climate zones and biomes indicated their uneven temperature sensitivities
to future climate change, challenging the perspective that the parameters of global carbon stimulation
440 independent on climate zones and biomes; (3) precipitation dominated the spatial variabilities of RA.
However, further improvements in the approach should overcome shortcomings from reduced data
availability and the mismatch in spatial resolution between covariates and in situ RA.

Author contributions. XT, SF, WZ and SG designed the research and collected the data, XT, WZ and
SG contributed to the data processing and analysis. XT, WZ, SG, GC and LS wrote the manuscript, and
445 all authors contributed to the review the manuscript.

Competing interests. The authors declare that they have no conflict of interest.

Acknowledgements. This study was supported by Fundamental Research Funds of International Centre
for Bamboo and Rattan (1632017003 and 1632018003); the National Natural Science Foundation of
China (31800365); Innovation funding of Remote Sensing Science and Technology of Chengdu



450 University of Technology (KYTD201501); Starting Funding of Chengdu University of Technology
(10912-2018KYQD-06910) and Open Funding from Key Laboratory of Geoscience Spatial Information
Technology of Ministry of Land and Resources (Chengdu University of Technology). The authors
express their great thanks to the contributors of Hashimoto soil respiration dataset, the contributors of
collecting data from publication in SRDB. Great thanks to Dr. Shoji Hashimoto for his valuable
455 comments to improve the manuscript.

References

- Bodesheim, P., Jung, M., Gans, F., Mahecha, M. D., and Reichstein, M.: Upscaled diurnal cycles of land–
atmosphere fluxes: a new global half-hourly data product, *Earth Syst. Sci. Data*, 10, 1327-1365,
460 <http://dx.doi.org/10.5194/essd-10-1327-2018>, 2018.
- Bond-Lamberty, B., Bailey, V. L., Chen, M., Gough, C. M., and Vargas, R.: Globally rising soil
heterotrophic respiration over recent decades, *Nature*, 560, 80-83, [http://dx.doi.org/10.1038/s41586-018-
0358-x](http://dx.doi.org/10.1038/s41586-018-
0358-x), 2018.
- Bond-Lamberty, B. and Thomson, A.: A global database of soil respiration data, *Biogeosciences*, 7, 1915-
465 1926, <http://dx.doi.org/10.5194/bg-7-1915-2010>, 2010a.
- Bond-Lamberty, B. and Thomson, A.: Temperature-associated increases in the global soil respiration
record, *Nature*, 464, 579-582, <http://dx.doi.org/10.1038/nature08930>, 2010b.
- Bond-Lamberty, B., Wang, C., and Gower, S. T.: A global relationship between the heterotrophic and
autotrophic components of soil respiration?, *Glob. Chang. Biol.*, 10, 1756-1766,
470 <http://dx.doi.org/10.1111/j.1365-2486.2004.00816.x>, 2004.
- Breiman, L.: Random forests, *Mach. Learn.*, 45, 5-32, <http://dx.doi.org/10.1023/A:1010933404324>, 2001.
- Chen, G. S., Yang, Y. S., and Robinson, D.: Allometric constraints on, and trade-offs in, belowground
carbon allocation and their control of soil respiration across global forest ecosystems, *Glob. Chang. Biol.*,
20, 1674-1684, <http://dx.doi.org/10.1111/gcb.12494>, 2014.
- 475 Feng, H. H. and Liu, Y. B.: Combined effects of precipitation and air temperature on soil moisture in
different land covers in a humid basin, *J. Hydrol.*, 531, 1129-1140,
<http://dx.doi.org/10.1016/j.jhydrol.2015.11.016>, 2015.
- Forkel, M., Carvalhais, N., Rödenbeck, C., Keeling, R., Heimann, M., Thonicke, K., Zaehle, S., and



- Reichstein, M.: Enhanced seasonal CO₂ exchange caused by amplified plant productivity in northern
480 ecosystems, *Science*, 351, 696-699, <http://dx.doi.org/10.1126/science.aac4971>, 2016.
- Gauchere, C., Alleaume, S., and Hely, C.: The comparison map profile method: a strategy for multiscale
comparison of quantitative and qualitative images, *IEEE Trans. Geosci. Remote Sens.*, 46, 2708-2719,
<http://dx.doi.org/10.1109/TGRS.2008.919379>, 2008.
- Gomez-Casanovas, N., Matamala, R., Cook, D. R., and Gonzalez-Meler, M. A.: Net ecosystem exchange
485 modifies the relationship between the autotrophic and heterotrophic components of soil respiration with
abiotic factors in prairie grasslands, *Glob. Chang. Biol.*, 18, 2532-2545, <http://dx.doi.org/10.1111/j.1365-2486.2012.02721.x>, 2012.
- Gray, S. B., Dermody, O., Klein, S. P., Locke, A. M., McGrath, J. M., Paul, R. E., Rosenthal, D. M., Ruiz-
Vera, U. M., Siebers, M. H., Strellner, R., Ainsworth, E. A., Bernacchi, C. J., Long, S. P., Ort, D. R., and
490 Leakey, A. D. B.: Intensifying drought eliminates the expected benefits of elevated carbon dioxide for
soybean, *Nature Plants*, 2, 16132, <http://dx.doi.org/10.1038/nplants.2016.132>, 2016.
- Högberg, P., Nordgren, A., and Ågren, G.: Carbon allocation between tree root growth and root
respiration in boreal pine forest, *Oecologia*, 132, 579-581, <http://dx.doi.org/10.1007/s00442-002-0983-8>, 2002.
- 495 Högberg, P., Nordgren, A., Buchmann, N., Taylor, A. F. S., Ekblad, A., Hogberg, M. N., Nyberg, G.,
Ottosson-Lofvenius, M., and Read, D. J.: Large-scale forest girdling shows that current photosynthesis
drives soil respiration, *Nature*, 411, 789-792, <http://dx.doi.org/10.1038/35081058>, 2001.
- Hansen, M. C., Potapov, P. V., Moore, R., Hancher, M., Turubanova, S. A., Tyukavina, A., Thau, D.,
Stehman, S. V., Goetz, S. J., Loveland, T. R., Kommareddy, A., Egorov, A., Chini, L., Justice, C. O., and
500 Townshend, J. R. G.: High-Resolution Global Maps of 21st-Century Forest Cover Change, *Science*, 342,
850-853, <http://dx.doi.org/10.1126/science.1244693>, 2013.
- Hanson, P. J., Edwards, N. T., Garten, C. T., and Andrews, J. A.: Separating root and soil microbial
contributions to soil respiration: A review of methods and observations, *Biogeochemistry*, 48, 115-146,
<http://dx.doi.org/10.1023/a:1006244819642>, 2000.
- 505 Harris, I., Jones, P., Osborn, T., and Lister, D.: Updated high - resolution grids of monthly climatic
observations—the CRU TS3.10 Dataset, *Int. J. Climatol.*, 34, 623-642, <http://dx.doi.org/10.1002/joc.3711>,
2014.
- Hashimoto, S., Carvalhais, N., Ito, A., Migliavacca, M., Nishina, K., and Reichstein, M.: Global



- spatiotemporal distribution of soil respiration modeled using a global database, *Biogeosciences*, 12,
510 4121–4132, <http://dx.doi.org/10.5194/bgd-12-4331-2015>, 2015.
- Hengl, T., Mendes de Jesus, J., Heuvelink, G. B., Ruiperez Gonzalez, M., Kilibarda, M., Blagotic, A.,
Shangguan, W., Wright, M. N., Geng, X., Bauer-Marschallinger, B., Guevara, M. A., Vargas, R.,
MacMillan, R. A., Batjes, N. H., Leenaars, J. G., Ribeiro, E., Wheeler, I., Mantel, S., and Kempen, B.:
SoilGrids250m: Global gridded soil information based on machine learning, *PLoS One*, 12, e0169748,
515 <http://dx.doi.org/10.1371/journal.pone.0169748>, 2017.
- Hursh, A., Ballantyne, A., Cooper, L., Maneta, M., Kimball, J., and Watts, J.: The sensitivity of soil
respiration to soil temperature, moisture, and carbon supply at the global scale, *Glob. Chang. Biol.*, 23,
2090-2103, <http://dx.doi.org/10.1111/gcb.13489>, 2017.
- IPCC: Climate Change 2013: The Physical Science Basis. Contribution of Working Group I to the Fifth
520 Assessment Report of the Intergovernmental Panel on Climate Change, Cambridge University Press,
Cambridge, United Kingdom and New York, NY, USA, 2013.
- Jian, J., Steele, M. K., Thomas, R. Q., Day, S. D., and Hodges, S. C.: Constraining estimates of global
soil respiration by quantifying sources of variability, *Glob. Chang. Biol.*, 24, 4143-4159,
<http://dx.doi.org/10.1111/gcb.14301>, 2018.
- 525 Jung, M., Reichstein, M., Schwalm, C. R., Huntingford, C., Sitch, S., Ahlstrom, A., Arneeth, A., Camps-
Valls, G., Ciais, P., Friedlingstein, P., Gans, F., Ichii, K., Jain, A. K., Kato, E., Papale, D., Poulter, B.,
Raduly, B., Rodenbeck, C., Tramontana, G., Viovy, N., Wang, Y. P., Weber, U., Zaehle, S., and Zeng, N.:
Compensatory water effects link yearly global land CO₂ sink changes to temperature, *Nature*, 541, 516-
520, <http://dx.doi.org/10.1038/nature20780>, 2017.
- 530 Kabacoff, R. I.: *R in action: data analysis and graphics with R*, Manning Publications Co., Shelter Island,
New York, 2015.
- Kalnay, E., Kanamitsu, M., Kistler, R., Collins, W., Deaven, D., Gandin, L., Iredell, M., Saha, S., White,
G., Woollen, J., Zhu, Y., Chelliah, M., Ebisuzaki, W., Higgins, W., Janowiak, J., Mo, K. C., Ropelewski,
C., Wang, J., Leetmaa, A., Reynolds, R., Jenne, R., and Joseph, D.: The NCEP/NCAR 40-year reanalysis
535 project, *Bull. Am. Meteorol. Soc.*, 77, 437-471, [http://dx.doi.org/10.1175/1520-0477\(1996\)077<0437:Tnyrp>2.0.Co;2](http://dx.doi.org/10.1175/1520-0477(1996)077<0437:Tnyrp>2.0.Co;2), 1996.
- Klein Goldewijk, K., Beusen, A., Van Drecht, G., and De Vos, M.: The HYDE 3.1 spatially explicit
database of human-induced global land-use change over the past 12,000 years, *Global Ecol. Biogeogr.*,



- 20, 73-86, <http://dx.doi.org/10.1111/j.1466-8238.2010.00587.x>, 2011.
- 540 Kuzyakov, Y. and Gavrichkova, O.: Time lag between photosynthesis and carbon dioxide efflux from soil: a review of mechanisms and controls, *Glob. Chang. Biol.*, 16, 3386-3406, <http://dx.doi.org/10.1111/j.1365-2486.2010.02179.x>, 2010.
- Le Quéré, C., Andrew, R. M., Friedlingstein, P., Sitch, S., Pongratz, J., Manning, A. C., Korsbakken, J. I., Peters, G. P., Canadell, J. G., Jackson, R. B., Boden, T. A., Tans, P. P., Andrews, O. D., Arora, V. K.,
- 545 Bakker, D. C. E., Barbero, L., Becker, M., Betts, R. A., Bopp, L., Chevallier, F., Chini, L. P., Ciais, P., Cosca, C. E., Cross, J., Currie, K., Gasser, T., Harris, I., Hauck, J., Haverd, V., Houghton, R. A., Hunt, C. W., Hurtt, G., Ilyina, T., Jain, A. K., Kato, E., Kautz, M., Keeling, R. F., Klein Goldewijk, K., Körtzinger, A., Landschützer, P., Lefèvre, N., Lenton, A., Lienert, S., Lima, I., Lombardozzi, D., Metzl, N., Millero, F., Monteiro, P. M. S., Munro, D. R., Nabel, J. E. M. S., Nakaoka, S.-i., Nojiri, Y., Padín, X. A., Pregon,
- 550 A., Pfeil, B., Pierrot, D., Poulter, B., Rehder, G., Reimer, J., Rödenbeck, C., Schwinger, J., Séférian, R., Skjelvan, I., Stocker, B. D., Tian, H., Tilbrook, B., van der Laan-Luijckx, I. T., van der Werf, G. R., van Heuven, S., Viovy, N., Vuichard, N., Walker, A. P., Watson, A. J., Wiltshire, A. J., Zaehle, S., and Zhu, D.: Global Carbon Budget 2017, *Earth System Science Data Discussions*, 10, 1-79, [10.5194/essd-2017-123](https://doi.org/10.5194/essd-2017-123), 2017.
- 555 Li, P., Peng, C., Wang, M., Li, W., Zhao, P., Wang, K., Yang, Y., and Zhu, Q.: Quantification of the response of global terrestrial net primary production to multifactor global change, *Ecol. Indic.*, 76, 245-255, <http://dx.doi.org/10.1016/j.ecolind.2017.01.021>, 2017.
- Liu, Y., Liu, S., Wan, S., Wang, J., Luan, J., and Wang, H.: Differential responses of soil respiration to soil warming and experimental throughfall reduction in a transitional oak forest in central China, *Agric. For. Meteorol.*, 226, 186-198, <http://dx.doi.org/10.1016/j.agrformet.2016.06.003>, 2016.
- 560 Moyano, F. E., Vasilyeva, N., Bouckaert, L., Cook, F., Craine, J., Curiel Yuste, J., Don, A., Epron, D., Formanek, P., Franzluebbers, A., Ilstedt, U., Kätterer, T., Orchard, V., Reichstein, M., Rey, A., Ruamps, L., Subke, J. A., Thomsen, I. K., and Chenu, C.: The moisture response of soil heterotrophic respiration: interaction with soil properties, *Biogeosciences*, 9, 1173-1182, <http://dx.doi.org/10.5194/bg-9-1173-2012>,
- 2012.
- Peel, M. C., Finlayson, B. L., and McMahon, T. A.: Updated world map of the Köppen-Geiger climate classification, *Hydrol. Earth Syst. Sci.*, 11, 1633-1644, <http://dx.doi.org/10.5194/hess-11-1633-2007>, 2007.



- 570 Piñeiro, J., Ochoa-Hueso, R., Delgado-Baquerizo, M., Dobrick, S., Reich, P. B., Pendall, E., and Power, S. A.: Effects of elevated CO₂ on fine root biomass are reduced by aridity but enhanced by soil nitrogen: A global assessment, *Sci. Rep.*, 7, 15355, <http://dx.doi.org/10.1038/s41598-017-15728-4>, 2017.
- Pumpanen, J., Kolari, P., Ilvesniemi, H., Minkkinen, K., Vesala, T., Niinistö, S., Lohila, A., Larmola, T., Morero, M., Pihlatie, M., Janssens, I., Yuste, J. C., Grünzweig, J. M., Reth, S., Subke, J.-A., Savage, K., Kutsch, W., Østreg, G., Ziegler, W., Anthoni, P., Lindroth, A., and Hari, P.: Comparison of different
575 chamber techniques for measuring soil CO₂ efflux, *Agric. For. Meteorol.*, 123, 159-176, <http://dx.doi.org/10.1016/j.agrformet.2003.12.001>, 2004.
- Raich, J. W. and Schlesinger, W. H.: The global carbon dioxide flux in soil respiration and its relationship to vegetation and climate, *Tellus B*, 44, 81-99, <http://dx.doi.org/10.1034/j.1600-0889.1992.t01-1-00001.x>, 1992.
- 580 Reichstein, M., Papale, D., Valentini, R., Aubinet, M., Bernhofer, C., Knohl, A., Laurila, T., Lindroth, A., Moors, E., Pilegaard, K., and Seufert, G.: Determinants of terrestrial ecosystem carbon balance inferred from European eddy covariance flux sites, *Geophys. Res. Lett.*, 34, L01402, <http://dx.doi.org/10.1029/2006GL027880>, 2007.
- Schaefer, D. A., Feng, W., and Zou, X.: Plant carbon inputs and environmental factors strongly affect soil
585 respiration in a subtropical forest of southwestern China, *Soil Biol. Biochem.*, 41, 1000-1007, <http://dx.doi.org/10.1016/j.soilbio.2008.11.015>, 2009.
- Subke, J.-A., Voke, N. R., Leronni, V., Garnett, M. H., and Ineson, P.: Dynamics and pathways of autotrophic and heterotrophic soil CO₂ efflux revealed by forest girdling, *J. Ecol.*, 99, 186-193, <http://dx.doi.org/10.1111/j.1365-2745.2010.01740.x>, 2011.
- 590 Tang, X., Fan, S., Qi, L., Guan, F., Du, M., and Zhang, H.: Soil respiration and net ecosystem production in relation to intensive management in Moso bamboo forests, *Catena*, 137, 219-228, <http://dx.doi.org/10.1016/j.catena.2015.09.008>, 2016.
- Tang, X., Fan, S., Zhang, W., Gao, S., Chen, G., and Shi, L.: Global variability of belowground autotrophic respiration in terrestrial ecosystems, *Figshare*, <https://doi.org/10.6084/m9.figshare.7636193>,
595 2019.
- Tian, X., Yan, M., van der Tol, C., Li, Z., Su, Z., Chen, E., Li, X., Li, L., Wang, X., Pan, X., Gao, L., and Han, Z.: Modeling forest above-ground biomass dynamics using multi-source data and incorporated models: A case study over the qilian mountains, *Agric. For. Meteorol.*, 246, 1-14,



- <http://dx.doi.org/10.1016/j.agrformet.2017.05.026>, 2017.
- 600 Wang, C. and Yang, J.: Rhizospheric and heterotrophic components of soil respiration in six Chinese temperate forests, *Glob. Chang. Biol.*, 13, 123-131, <http://dx.doi.org/10.1111/j.1365-2486.2006.01291.x>, 2007.
- Wang, X., Liu, L., Piao, S., Janssens, I. A., Tang, J., Liu, W., Chi, Y., Wang, J., and Xu, S.: Soil respiration under climate warming: differential response of heterotrophic and autotrophic respiration, *Glob. Chang. Biol.*, 20, 3229-3237, <http://dx.doi.org/10.1111/gcb.12620>, 2014.
- 605 Yan, M. F., Zhou, G. S., and Zhang, X. S.: Effects of irrigation on the soil CO₂ efflux from different poplar clone plantations in arid northwest China, *Plant Soil*, 375, 89-97, <http://dx.doi.org/10.1007/s11104-013-1944-1>, 2014.
- Yao, Y., Wang, X., Li, Y., Wang, T., Shen, M., Du, M., He, H., Li, Y., Luo, W., Ma, M., Ma, Y., Tang, Y.,
- 610 Wang, H., Zhang, X., Zhang, Y., Zhao, L., Zhou, G., and Piao, S.: Spatiotemporal pattern of gross primary productivity and its covariation with climate in China over the last thirty years, *Glob. Chang. Biol.*, 24, 184-196, <http://dx.doi.org/10.1111/gcb.13830>, 2018.
- Zhang, Y., Xiao, X., Wu, X., Zhou, S., Zhang, G., Qin, Y., and Dong, J.: A global moderate resolution dataset of gross primary production of vegetation for 2000–2016, *Sci. Data*, 4, 170165, <http://dx.doi.org/10.1038/sdata.2017.165>, 2017.
- 615 Zhao, Z., Peng, C., Yang, Q., Meng, F.-R., Song, X., Chen, S., Epule, T. E., Li, P., and Zhu, Q.: Model prediction of biome-specific global soil respiration from 1960 to 2012, *Earth's Future*, 5, 715-729, <http://dx.doi.org/10.1002/2016EF000480>, 2017.
- Zhou, L., Zhou, X., Shao, J., Nie, Y., He, Y., Jiang, L., Wu, Z., and Hosseini Bai, S.: Interactive effects
- 620 of global change factors on soil respiration and its components: a meta-analysis, *Glob. Chang. Biol.*, 22, 3157-3169, <http://dx.doi.org/10.1111/gcb.13253>, 2016.

623